Taylor & Francis
Taylor & Francis Group

BASIC RESEARCH PAPER

🔓 OPEN ACCESS

HLH-30/TFEB-mediated autophagy functions in a cell-autonomous manner for epithelium intrinsic cellular defense against bacterial pore-forming toxin in *C. elegans*

Huan-Da Chen[a,b], Cheng-Yuan Kao[c], Bang-Yu Liu[a], Shin-Whei Huang[a], Cheng-Ju Kuo[a,b], Jhen-Wei Ruan[c], Yen-Hung Lin[d], Cheng-Rung Huang[a], Yu-Hung Chen[a,e], Horng-Dar Wang[d], Raffi V. Aroian[f], and Chang-Shi Chen[a,b]

[a]Department of Biochemistry and Molecular Biology, College of Medicine, National Cheng Kung University, Tainan, Taiwan; [b]Institute of Basic Medical Sciences, College of Medicine, National Cheng Kung University, Tainan, Taiwan; [c]Immunology Research Center, National Health Research Institutes, Miaoli, Taiwan; [d]Institute of Biotechnology, National Tsing Hua University, Hsinchu, Taiwan; [e]School of Medicine, College of Medicine, National Cheng Kung University, Tainan, Taiwan; [f]Program in Molecular Medicine, University of Massachusetts Medical School, Worcester, MA, USA

ABSTRACT

Autophagy is an evolutionarily conserved intracellular system that maintains cellular homeostasis by degrading and recycling damaged cellular components. The transcription factor HLH-30/TFEB-mediated autophagy has been reported to regulate tolerance to bacterial infection, but less is known about the *bona fide* bacterial effector that activates HLH-30 and autophagy. Here, we reveal that bacterial membrane pore-forming toxin (PFT) induces autophagy in an HLH-30-dependent manner in *Caenorhabditis elegans*. Moreover, autophagy controls the susceptibility of animals to PFT toxicity through xenophagic degradation of PFT and repair of membrane-pore cell-autonomously in the PFT-targeted intestinal cells in *C. elegans*. These results demonstrate that autophagic pathways and autophagy are induced partly at the transcriptional level through HLH-30 activation and are required to protect metazoan upon PFT intoxication. Together, our data show a new and powerful connection between HLH-30-mediated autophagy and epithelium intrinsic cellular defense against the single most common mode of bacterial attack in vivo.

Introduction

Many bacterial pathogens, both Gram-positive and -negative, produce pore-forming toxins (PFTs) that damage the plasma membrane of host cells and are of importance to infection and pathogenesis.[1,2] PFTs that contribute significantly to bacterial virulence include streptolysin O (SLO) from human-pathogenic Streptococci and crystal (Cry) toxins by *Bacillus thuringiensis* (Bt). The importance of PFTs in promoting bacterial pathogenesis has been demonstrated in numerous experiments where individual PFTs have been genetically mutated from pathogenic bacteria and the mutants then tested for attenuated or even no virulence. However, functional analyses of the epithelium <u>in</u>trinsic <u>ce</u>llular <u>de</u>fense (INCED) of the host at the organismal level to this largest class of bacterial virulence factors remains a vastly understudied area.[3]

Bt Cry toxins, including Cry5B and Cry21A that were used in this study, can intoxicate a wide range of plant-parasitic, animal-parasitic, and free-living nematodes, including the standard laboratory species, *C. elegans*.[4] This Cry toxin–*C. elegans* interaction system has opened up the first whole-animal genetic model for studying PFTs in vivo and has led to the discovery of several important INCED (PFT defense) pathways, including MAPK/JNK/p38 (mitogen-activated protein kinase) pathways,[5,6] unfolded protein response (UPR) pathways,[7] the hypoxia pathway,[8] the DAF-2 insulin-like pathways,[3] and the RAB-5 and RAB-11-dependent vesicle-trafficking pathways.[9] All these pathways protect *C. elegans* against Cry and other PFTs and in many cases, show parallel responses in mammalian cells under attack by PFTs.

Autophagy is an evolutionarily conserved cellular catabolic process involved in the formation of phagophores, double-membrane compartments that are responsible for removing aggregation-prone proteins or superfluous and damaged organelles through the formation of an autophagosome and the autophagosomal-lysosomal pathway.[10] In higher eukaryotes, autophagy can be induced when cells are under metabolic stress, undergoing cellular remodeling, or removing damaged cellular constituents, therefore with an astonishing number of connections to development and normal physiology.[11] Moreover, autophagy has been linked to a wide range of human pathologies, including infection, immunity, and inflammatory diseases.[12,13] Genetic screens, primarily in yeast, have identified more than 40 autophagy-related (*ATG*) genes.[14] Many of these genes have orthologs in higher eukaryotes, including *C. elegans* and mammals. Genetic manipulations of *ATG* ortholog genes in *C. elegans* have been very useful to probe the functions of autophagy in an intact multicellular organism during development.[15,16]

CONTACT Chang-Shi Chen ✉ cschen@mail.ncku.edu.tw 📍 1 University Road, Tainan 70101, Taiwan.

Color versions of one or more of the figures in the article can be found online at www.tandfonline.com/kaup.

Supplemental data for this article can be accessed on the publisher's website.

Many of the key signal modulators for autophagy regulation in other eukaryotic organisms appear to be conserved in *C. elegans*. Recent reports suggested that the transcription factor HLH-30 (TFEB in mammals) regulates autophagy activation in nutrient availability, lifespan regulation, and *Staphylococcus aureus* infection.[17-20] Moreover, autophagy has been reported to control the susceptibility of mammalian cells to various PFTs, including *V. cholerae* cytolysin (VCC) and α-hemolysin (α-toxin, Hla) by *S. aureus*,[21-23] but how autophagy is triggered and its role at the organismal level are still largely understudied.

Cry5B perforates the intestinal cells via binding to the host glycosphingolipid receptors made by at least 4 glycosyltransferases encoded by *bre* (Bt toxin-resistant) genes in *C. elegans*.[24] Animals fed Cry5B show extensive cellular morphological changes, including the formation of vacuole-like structures in gut cells.[25] In a rhodamine-labeled Cry5B feeding experiment in *C. elegans*,[24] image analysis data show that although the majority of the Cry5B toxin signals are located in the intestinal lumen and on the apical surface of the intestinal cells, gut cells internalize some Cry5B or Cry5B fragments. Moreover, Cry5B toxin signals form multiple cytosolic puncta after being internalized into intestinal cells. All these features are reminiscent of the characteristics of cellular autophagy. Therefore, we designed in vivo experiments to determine the roles of autophagy in epithelium INCED against pore-forming toxins in *C. elegans*.

Results

Pore-forming toxin Cry5B activates autophagy in C. elegans

To determine whether autophagy plays roles in Cry5B PFT intoxication or defense, we analyzed previous microarray data of the Cry5B-*C. elegans* interaction,[5,6] and found several *atg* genes (*unc-51, lgg-1, lgg-2, lgg-3, atg-3,* and *atg-18*) which were significantly upregulated after 3 h of exposure to Cry5B. This result suggested that Cry5B could activate transcription of these genes, or even cellular autophagy. We therefore performed quantitative real-time RT-PCR (qRT-PCR) to reconfirm the transcriptional activation of these genes after Cry5B exposure in *glp-4(bn2)* animals, the same *C. elegans* strain as used in the microarray studies (Fig. 1A). Our results showed that transcription of 4 out of the 6 genes identified in the transcriptomic analysis, *lgg-1, lgg-2, lgg-3,* and *atg-18*, was significantly upregulated by Cry5B (all *P* < 0.01); however, the transcription of *unc-51* (0.82×) and *atg-3* (0.73×) were not upregulated in our qRT-PCR analysis.

To independently reconfirm that Cry5B upregulates the expression of *atg* genes, including *lgg-1* and to test if Cry5B activates cellular autophagy, we examined the expression level and posttranslational modification of the LGG-1 protein in the wild-type N2 animals by western blot (Fig. 1B, quantified in Fig. 1C). The quantitative results not only showed that total LGG-1 proteins (both LGG-1-I and LGG-1-II) increased significantly after Cry5B treatment (*P* < 0.01), but also demonstrated that the protease-cleaved and phosphatidylethanolamine (PE)-conjugated LGG-1-II, which is a marker for the activation of cellular autophagy,[26] significantly increased in the Cry5B-treated animals (*P* < 0.01).

To reconfirm the upregulation of *lgg-1* independently and to monitor the activation site of cellular autophagy induced by Cry5B in *C. elegans*, we fed DA2123 transgenic animals, carrying the *lgg-1p::GFP::lgg-1* reporter, on Cry5B-expressing *E. coli* plates for 3 h. The green fluorescence signal of GFP::LGG-1 was significantly increased in animals feeding on Cry5B plates (*P* < 0.01) compare with those on control plates (Fig. 1D and E), which is consistent with the LGG-1 western blot analysis (Fig. 1B and C). Notably, the GFP::LGG-1 signals were predominantly enhanced and formed multiple cellular puncta, the intracellular biomarkers for the phagophore and autophagosomal membranes,[26] in the intestinal cells (Fig. 1D). The Cry5B-treated animals had significant intestinal multiple cellular GFP::LGG-1 puncta (*P* < 0.01) compare with the control group (Fig. 1F). Moreover, the average GFP::LGG-1 puncta or foci number in the Int1 (the first anterior ring of intestine) cells was significantly increased in the Cry5B-treated group (*P* < 0.01) (Fig. 1G). However, defect of normal autophagic flux may also result in the accumulation of GFP::LGG-1 foci number. In order to test whether Cry5B can activate or inhibit autophagic flux, the autophagic flux reporter HZ946 *rpl-43(bp399);bpIs151 (SQST-1::GFP)* animals were used.,[26,27] In the *rpl-43* hypomorphic mutant background, the autophagy substrate SQST-1:: GFP proteins are not degraded by autophagy and show aggregated signals in the intestinal cells. However, the Cry5B-treated animals had significantly less intestinal SQST-1::GFP aggregates compare with the untreated control group (Fig. 1H and I). Together, our results were consistent with the fact that Cry5B activates autophagy in the intestinal cells, the main targets of Cry5B.

We next tested whether these transcriptionally activated *atg* genes are required for Cry5B-induced autophagy. To this end, we subjected DA2123 animals to both Cry5B- and RNAi-expressing *E. coli*, and examined the formation of the intestinal multiple cellular GFP::LGG-1 puncta in these animals. When DA2123 animals were fed on Cry5B plates containing *atg* gene RNAi, the percentage of animals positive for intestinal GFP::LGG-1 puncta significantly decreased in the animals with knockdown of *lgg-1, lgg-2, lgg-3,* and *atg-18* compare with the L4440 RNAi vector control group (all *P* < 0.01) (Fig. S1A and B). Interestingly, RNAi of the *atg-18* gene not only abolished the formation of Cry5B-induced GFP::LGG-1 puncta but also the GFP::LGG-1 signals in the intestine of *C. elegans* (Fig. S1A). Nevertheless, our results here demonstrated that these Cry5B upregulated *atg* genes are required for autophagy activation in the Cry5B-targeted intestinal cells. Notably, several general cellular stressors, including heavy metal (10 mM Cu^{2+}), osmotic pressure (400 mM NaCl), heat shock (35°C), and non-PFT producing pathogen (*Pseudomonas aeruginosa* PA14),[7] did not activate intestinal GFP::LGG-1 puncta in DA2123 animals within 3 h (Fig. S2), suggesting the activation of autophagy by Cry5B is relatively specific to the action of PFT, at least in this time frame, but not the other cellular stresses.

To observe the Cry5B PFT-induced autophagy at more detailed anatomic level, we examined the Cry5B-targeted intestinal cells by TEM analysis. In addition to the intestinal microvilli shedding induced by Cry5B,[9] our TEM analysis also demonstrated that double-membrane vehicles, probably autophagosomes, in the intestinal cells were significantly increased in N2 animals fed on Cry5B plates (*P* < 0.01) compare with those on control plates (Fig. 1J–L). All of these results together
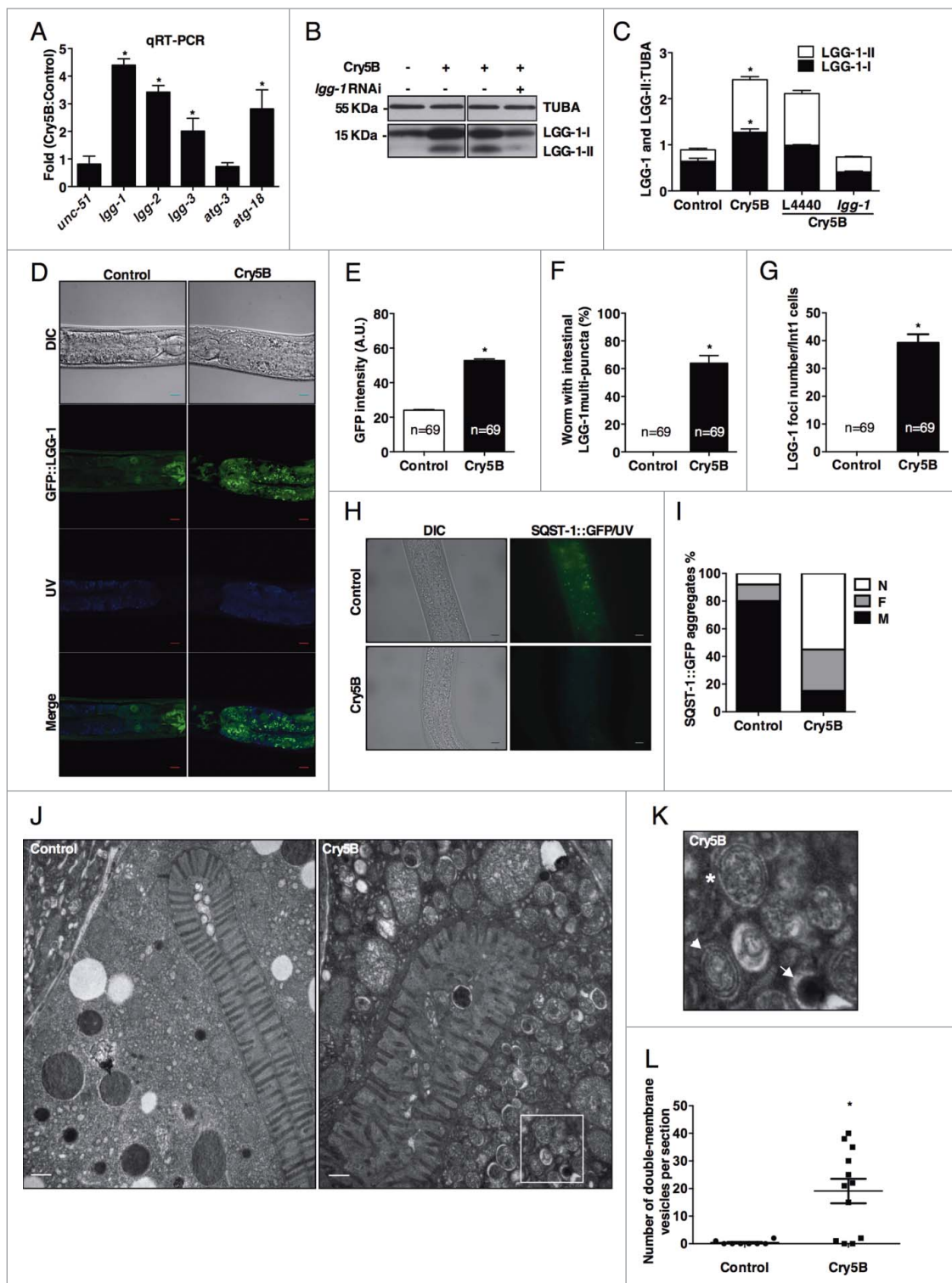
Figure 1. Autophagy is activated by Cry5B PFT in the intestine of *C. elegans*. (A) qRT-PCR analysis of Cry5B-activated *atg* genes in the *glp-4(bn2)* mutant. (B) Representative western blot for the expression level and posttranslational modification of LGG-1 in N2 animals treated with Cry5B. Signals for TUBA/α-tubulin were used as a loading control. The specificity of LGG-1 antibody was confirmed by *lgg-1* RNAi. (C) Quantitative analysis of 3 independent WB results. L4440 indicates RNAi control. (D) Representative DIC and confocal images of the DA2123 [*lgg-1p::GFP::lgg-1*] transgenic animals feeding on either Cry5B plates (Cry5B, right panels) or control OP50 plates (control, left panels) for 3 h. The confocal images of the GFP::LGG-1 signals (GFP::LGG-1, in green) and the autofluorescence signals (UV, in blue), and the 2 overlaid fluorescence images (Merge) and the differential interference contrast (DIC) images were presented. Scale bars: 10 μm. (E) Quantitative analysis of total green fluorescence signal of GFP::LGG-1. (F) Quantitative analysis of animals with intestinal GFP::LGG-1 cytosolic puncta. (G) Quantitative analysis of the GFP::LGG-1 foci number in the Int1 intestinal cells. (H) Representative DIC and epifluorescent images of the HZ946 *rpl-43(bp399);bpIs151(SQST-1::GFP)* animals feeding on either Cry5B plates (Cry5B, lower panels) or control OP50 plates (control, upper panels) for 3 h. The images of the SQST-1::GFP signals (SQST-1::GFP, in green) and the autofluorescence signals (UV, in blue) were overlaid (SQST-1::GFP/UV), and DIC were also presented. Scale bars: 10 μm. (I) Percentage of the animals with different levels of SQST-1::GFP aggregates. N indicates no or very low level of aggregates in intestinal cells; F indicates fewer aggregates in some but not all intestinal cells; M indicates many aggregates in all intestinal cells. (J) Representative TEM images of N2 animals fed with Cry5B or control. Scale bars: 0.5 μm. (K) Enlarged image of the white rectangular section in (J). Asterisk indicates a phagophore, arrowhead indicates an autophagosome, and arrow indicates an autolysosome. (L) Quantitative analysis of double-membrane vehicles identified. Error bars are SEM and n indicates total animals analyzed. *P < 0.05. A.U. arbitrary units. (See also Fig. S1 and S2.).

reveal that cellular autophagy is induced cell-autonomously by Cry5B, at least in part through transcriptional activation of the *atg* genes, *lgg-1*, *lgg-2*, *lgg-3*, and *atg-18*, in the Cry5B-targeted intestinal cells.

Autophagy is required for defense of *C. elegans* against Cry5B

Since autophagy can be prosurvival or prodeath in different cellular contexts,[28] we hypothesized that Cry5B, as well as forming pores at the plasma membrane, either exerts its toxicity through toxin internalization and induction of autophagic cell death (prodeath), or Cry5B-targeted cells mount INCED against it by activation of autophagy (prosurvival). To address this question, *C. elegans* with *atg* gene mutations, which cause autophagy defect at distinct regulatory steps, were quantitatively compare with wild-type N2 animals for susceptibility to Cry5B (Fig. 2A). The autophagic process can be dissected into distinct stages:[15] mammalian *BECN1/VPS30/ATG6* (*bec-1* in *C. elegans*) is required for the induction and vesicle nucleation stage; *ATG4* (*atg-4.1* and *atg-4.2* in *C. elegans*) encodes cysteine protease and mediates the vesicle expansion and completion; further, the retrieval of the integral membrane protein ATG-9 from the phagophore assembly site involves *atg-18*. These *atg* gene mutants, *bec-1(ok691)*, *bec-1(ok700)*, *atg-4.1(tm4364);atg-4.2 (tm3949)*, and *atg-18(gk378)* (except for the *atg-4.1(tm4364)* (*P* = 0.26) and *atg-4.2(tm3948)* (*P* = 0.42) single mutant) showed a significant Hpo (Hypersensitive to POre-forming toxin) phenotype to Cry5B killing compare with N2 animals (all *P* < 0.01). These data indicated that autophagy, controlled and regulated by these *atg* genes, was required for Cry5B

defense, and *atg-4.1* and *atg-4.2* function redundantly in the autophagy-dependent INCED against Cry5B intoxication.

To independently test that our results stem from loss-of-function phenotypes and reconfirm the importance of the transcriptional activation of autophagy in PFT responses, *atg* genes were silenced by RNAi in NL2099 *rrf-3(pk1426)* animals. Knockdown of the *atg* genes specifically activated by Cry5B, *lgg-1*, *lgg-2*, *lgg-3*, and *atg-18* (Fig. 2B), and the other *atg* gene *atg-10* which encodes a LGG-3/ATG12-conjugating enzyme and is essential for autophagic vesicle formation (Fig. S3A), all conferred a statistically significant Cry5B Hpo phenotype compare with the L4440 control group (all *P* < 0.01). We found that hypersensitivity to Cry5B as well as decreased intestinal GFP::LGG-1 multiple cellular puncta (Fig. S1) resulted from RNAi of *atg* genes, confirming that the Cry5B hyper-susceptibility correlated with a reduction of cellular autophagy.

We therefore tested whether induction of autophagy can protect *C. elegans* from Cry5B killing. Two independent transgenic strains overexpressing LGG-1 protein were used: DA2123 carries the chromosome-integrated transgene *adls2122[lgg-1p::GFP::lgg-1]* with lower extra copies of *lgg-1*; YW364 carries the extrachromosomal *lgg-1p::lgg-1* transgene with a comparative higher level of *lgg-1* (Fig. S3B). These were compared with N2 animals for their sensitivity to Cry5B (Fig. 2C). DA2123 and YW364 animals were significantly resistant to Cry5B compare with N2 animals (all *P* < 0.01). Moreover, YW364 animals were statistically more resistant to Cry5B than the DA2123 animals (*P* < 0.01). This result suggested gene dosage-dependence of *lgg-1* on INCED against Cry5B. We also knocked down the *atg* genes specifically activated by Cry5B in DA2123 animals. As shown in Figure S1, silencing these genes significantly abolished the Cry5B-activated autophagy in the intestinal cells of the DA2123 animals.
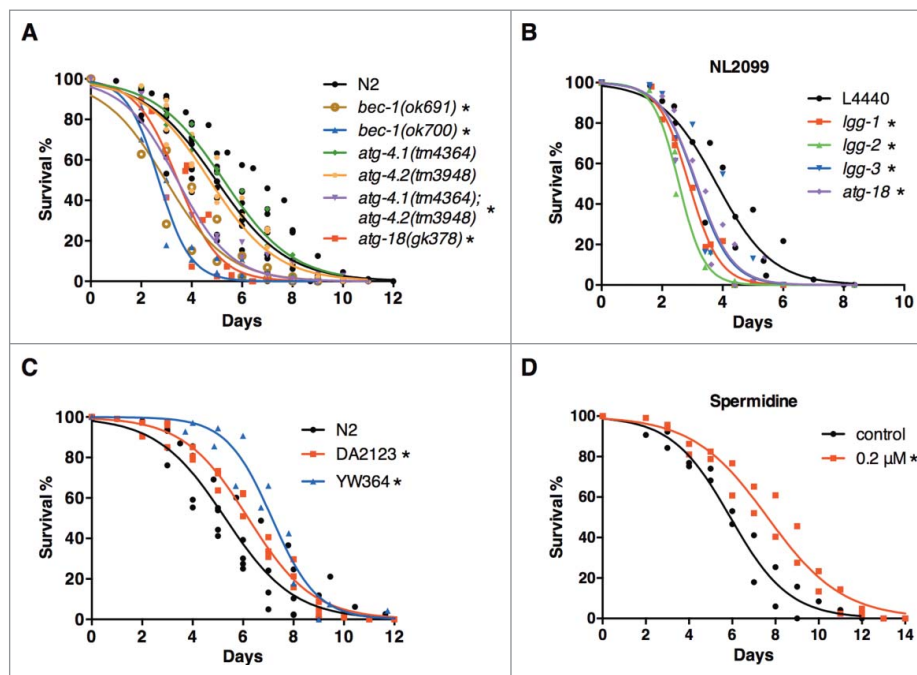

Figure 2. Autophagy controls the susceptibility to Cry5B PFT *in vivo*. (A) Survival analysis of N2, *bec-1(ok691)*, *bec-1(ok700)*, *atg-4.1(tm4364)*, *atg-4.2(tm3948)*, *atg-4.1 (tm4364);atg-4.2(tm3949)*, and *atg-18(gk378)* animals feeding on Cry5B plates. (B) Survival analysis of NL2099 *rrf-3(pk1426)* feeding on Cry5B- and RNAi-expressing *E. coli* plates. L4440 indicates the RNAi control-treated group. (C) Survival analysis of N2, DA2123 with *adls2122[lgg-1p:: GFP::lgg-1]*, and YW364 with extrachromosomal *lgg-1p:: lgg-1::GFP* transgene animals feeding on Cry5B plates. (D) Survival analysis of N2 animals on Cry5B plates with (0.2 µM) or without (control) spermidine. *P* < 0.05. (See also Figs. S3, S6, and S7.).

Moreover, RNAi of these *atg* genes, *lgg-1*, *lgg-2*, *lgg-3*, and *atg-18* (Fig. S3C), all significantly diminished the activated INCED against Cry5B compare with the L4440 control group in DA2123 animals (all *P* < 0.01). The results were in agreement with the findings that the activation of autophagy through the transcriptional upregulation of *lgg-1*, and the other *atg* genes, protected animals against Cry5B intoxication.

Pharmacological induction of autophagy, by spermidine,[29] was also independently tested (Fig. 2D). Animals on the plates containing the pharmacological autophagy inducer were more resistant to Cry5B than animals on the control plates (*P*< 0.01). The expression level of Cry5B in *E. coli* was not altered by spermidine at the same concentration (Fig. S3D and E). This indicated that the Cry5B resistance of the animals treated with spermidine on Cry5B-expressing *E. coli* plates was not due to a decrease in the total amount of Cry5B toxin on the plates. Together, our genetic and pharmacological analyses demonstrated that activation of autophagy is necessary and sufficient for INCED against Cry5B in *C. elegans*.

Autophagy functions cell-autonomously in the intestine to protect against Cry5B

Given that the membrane receptor for Cry5B PFT is expressed only on the intestinal cells of *C. elegans* and the formation of intestinal GFP::LGG-1 multiple cellular puncta induced by Cry5B was concomitantly observed, we hypothesized that autophagy functions cell-autonomously and is required in the intestine to protect against Cry5B intoxication in vivo. To genetically test this notion, we first silenced the Cry5B-activated *atg* genes specifically in the intestinal cells by feeding RNAi-expressing *E. coli* to VP303 [*rde-1(ne219);kbIs7(nhx-2p::rde-1)*] animals (Fig. 3A), in which RNAi is active only in the intestinal cells.[30] Intestine-specific knockdown of the Cry5B-activated *atg* genes, *lgg-1*, *lgg-2*, *lgg-3*, and *atg-18* all conferred a statistically significant Cry5B Hpo phenotype compare with the L4440 control (all *P* < 0.01).

To recapitulate the notion that cell-autonomous function of autophagy is required in the intestine for Cry5B defense, we
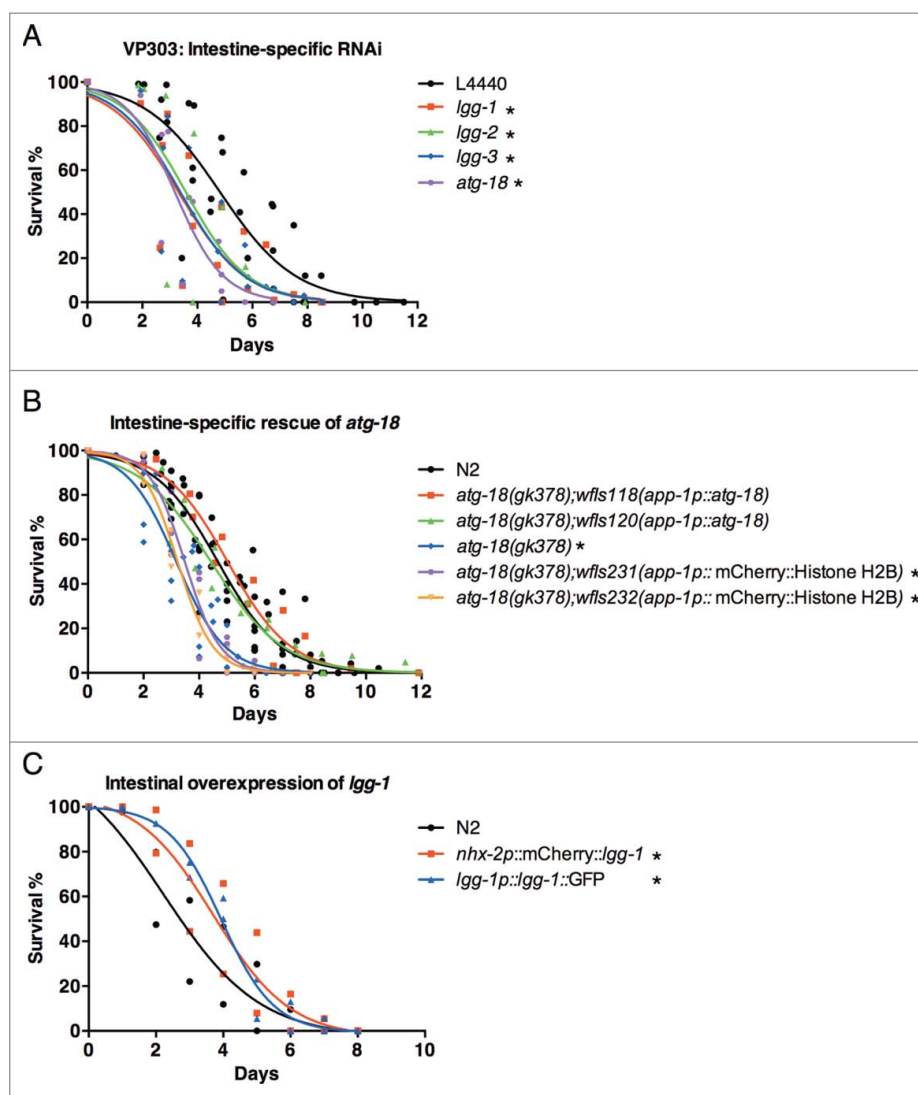

Figure 3. Autophagy functions cell-autonomously in the intestine for Cry5B PFT defense in *C. elegans*. (A) Survival analysis of VP303 [*rde-1(ne219);kbIs7(nhx-2p::rde-1)*] animals feeding on Cry5B- and RNAi-expressing *E. coli* plates. L4440 indicates the RNAi control-treated group. (B) Survival analysis of N2, YQ093 [*atg-18(gk378);wfIs118(app-1p::atg-18)*], YQ095 [*atg-18(gk378);wfIs120(app-1p::atg-18)*], *atg-18(gk378)*, YQ242 [*atg-18(gk378);wfIs231(app-1p:: mCherry::Histone H2B)*], and YQ243 [*atg-18(gk378); wfIs232(app-1p:: mCherry::Histone H2B)*] animals feeding on Cry5B plates. (C) Survival analysis of N2, VK1241 [*nhx-2p::mCherry::lgg-1*], and DA2123 [*lgg-1p::GFP::lgg-1*] animals feeding on Cry5B plates. *P<0.05. (See also Fig. S4.).

also generated 2 independent *C. elegans* strains, YQ093 [*atg-18 (gk378);wfIs118(app-1p::atg-18)*], and YQ095 [*atg-18(gk378); wfIs120(app-1p::atg-18)*], with specifically intestinal *atg-18* gene rescued driven by the *app-1* promoter in the *atg-18(gk378)* mutant background. The tissue specificity of the *app-1* promoter was also reconfirmed by monitoring the expression of *app-1p*-driven fluorescent reporter in the YQ242 [*atg-18 (gk378);wfIs231(app-1p::mCherry::Histone H2B)*] and YQ243 [*atg-18(gk378);wfIs232(app-1p::mCherry::Histone H2B)*] animals (Fig. S4A). While *atg-18(gk378)*, YQ242, and YQ243 animals were all significantly hypersensitive to Cry5B intoxication compare with the N2 animals (all *P* < 0.01), the YQ093 (*P* = 0.16) and YQ095 (*P* = 0.06) animals were as sensitive as N2 animals to Cry5B (Fig. 3B). Our data demonstrated that intestine-specific rescue of *atg-18* in the *atg-18(gk378)* mutant reverses its Cry5B Hpo phenotype.

To independently reconfirm the cell-autonomous function of autophagy in Cry5B defense, we also fed Cry5B to the VK1241 [*nhx-2p*::mCherry::*lgg-1*] transgenic animals, with intestine-specific overexpression of *lgg-1* driven by another intestine-specific promoter *nhx-2p*. Consistent with the previous results (Fig. 2C), the DA2123 animals with *lgg-1* overexpression driven by its endogenous promoter were more resistant to Cry5B toxicity compare with N2 animals (*P* < 0.01); while VK1241 animals were also significantly resistant to Cry5B compare with N2 (*P* < 0.01) and were as resistant as the DA2123 animals (*P* = 0.68) (Fig. 3C). Moreover, multiple mCherry::LGG-1 cellular puncta were also concomitantly observed in the intestinal cells of the Cry5B-treated VK1241 animals (Fig. S4B). Taking the above data together, we demonstrated that autophagy is activated and functions cell-autonomously for Cry5B defense in *C. elegans*.

Autophagy is involved in xenophagic degradation of PFT and membrane-pore repair

Cry5B binds to its glycosphingolipid receptor and thereafter forms pores on the cell membrane to intoxicate *C. elegans*.[24] However, when *C. elegans* was fed with the rhodamine-labeled Cry5B toxin (Rh-Cry5B), the Rh-Cry5B signals not only showed on the apical plasma membrane of the intestinal cells but also existed as multiple cellular puncta in the cytosol.[24] We repeated the experiments to reconfirm the results (Fig. S5A), i.e.-cytosolic Rh-Cry5B punctate signals were only seen with native and functional Cry5B in the intestinal cells with the presence of its receptor, but did not appear either in the *bre-3(ye28)* mutant without the Cry5B receptor or with the heat denatured Cry5B. Moreover, pore formation is required to induce autophagy by Cry5B, since *bre-3* is required for pore formation and RNAi of *bre-3* significantly diminishing the Cry5B-induced autophagy in DA2123 animals (Fig. S5B).

Given that the pattern of the cytosolic Rh-Cry5B signals (Fig. S5A) was reminiscent of Cry5B-induced multiple cytosolic LGG-1 cellular puncta as shown in Figure 1, and Figure S4, we tested to see whether the internalized Cry5B was degraded by xenophagy. First, by confocal microscopy, we found that the majority of the cytosolic Rh-Cry5B signals are colocalized with the punctate GFP::LGG-1 signals (autophagosomes), LysoTracker Blue signals (lysosomes), or both (autolysosomes) (Fig. 4A and B).

Next, by time-lapse image analysis, we determined whether Cry5B was degraded by autolysosomes. We found that cytosolic Rh-Cry5B signals are significantly diminished in the autolysosomes within 30 to 45 min (Fig. 4C). Taken together, our data suggests that the membrane pore-forming toxin Cry5B is, at least in part, degraded by autophagy in its target tissue, intestine.

Next we analyzed whether the clearance of Cry5B PFT in the intestinal cells can contribute to pore-repair on the apical plasma membrane. By using the membrane impermeable dye, propidium iodide (PI), which is smaller in size than the pore created by Cry5B, it is possible to qualify and quantify the intrinsic pore-repair activity in the intestinal cells of *C. elegans*.[9] After exposing of N2 animals to Cry5B for 0.5 h and chasing them briefly on non-Cry5B expressing *E. coli* plates for 0.5 h, PI was able to penetrate into the cytosol of intestinal cells in all Cry5B-treated groups (Fig. 5A). However, after 24 h of recovery on non-Cry5B expressing *E. coli* plates, PI signals were limited in the intestinal lumen and could not penetrate into the cytosol of intestinal cells in N2 animals treated with L4440 RNAi control. The results suggested an intrinsic membrane pore-repair activity in the Cry5B-targeted intestinal cells. Yet, when RNAi of the Cry5B-induced *atg* genes, *lgg-1, lgg-2, lgg-3*, and *atg-18*, the intrinsic membrane pore-repair activity is inhibited, since intestine cytosolic PI signals were detected in these *atg* RNAi-treated groups. Quantitative analysis also demonstrated that RNAi depletion of Cry5B-induced *atg* genes significantly abolished the pore-repair ratio, when compare with the animals treated with the control RNAi (L4440), examined 24 h after the recovery from Cry5B intoxication (all *P* < 0.01) (Fig. 5B). Together our data suggested that in addition to the endocytosis and exocytosis systems[9] autophagy also contributes to the intrinsic membrane pore-repair to defend against Cry5B PFT intoxication.

HLH-30 regulates the expression of Cry5B-activated *atg* genes

Next, we turned our attention to searching for the transcription factor that is activated by Cry5B and regulates these Cry5B-dependent *atg* genes, *lgg-1, lgg-2, lgg-3*, and *atg-18*. By *in silico* analysis, we identified 2 potential transcription factors, HLH-26 and HLH-30, which could regulate the transcription of these Cry5B-activated *atg* genes. The *cis*-regulatory consensus sequences and the potential binding sites for the HLH-26 and HLH-30 are illustrated in Figure 6A. To examine which transcription factor is required for the Cry5B-activated *atg* gene transcription, we knocked down *hlh-26* or *hlh-30* in the autophagy reporter DA2131 animals and fed them with Cry5B (Fig. 6B–E). Our results demonstrated that RNAi of *hlh-30* significantly abolished the Cry5B-induced autophagy in the intestinal cells, while RNAi of *hlh-26* had no effect. To reconfirm the roles of HLH-30, but not HLH-26, in Cry5B-activated autophagy and INCED against PFT intoxication, we fed the N2, *hlh-26(tm287)*, and *hlh-30(tm1978)* animals on Cry5B plates and monitored their susceptibility to PFT intoxication (Fig. 6F). Our results showed that only the *hlh-30(tm1978)* mutant is significantly hypersensitive to Cry5B toxicity compare with N2 (*P* < 0.01), while the *hlh-26(tm287)* mutant is as sensitive as N2 (*P* = 0.06).
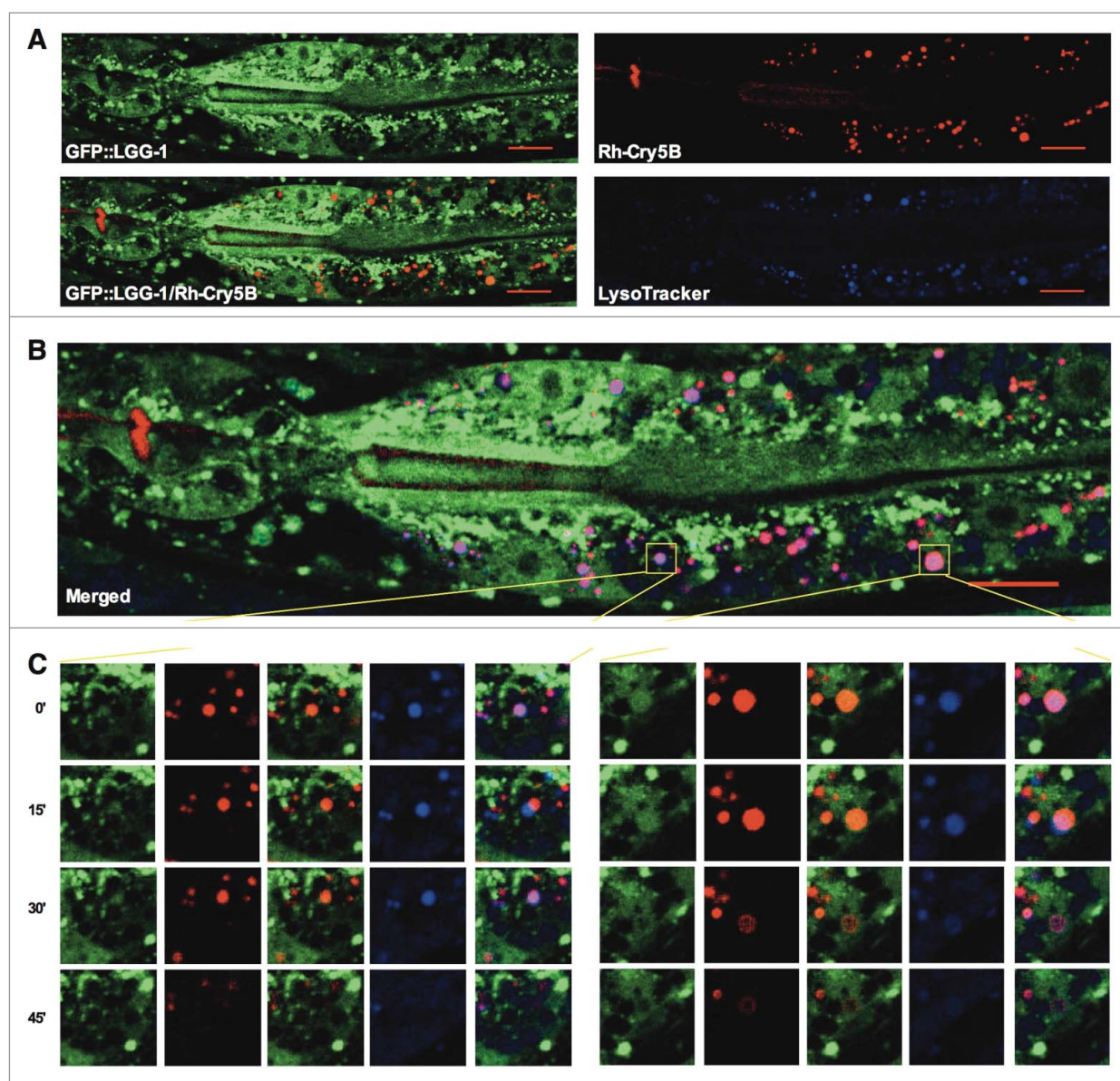
Figure 4. Autophagy plays a role in Cry5B PFT degradation (A) Confocal images of DA2123 animals fed with 50 μg/ml Rh-Cry5B for 3 h. (B) The enlarged image shows the merged signals of fluorescence images, Rh-Cry5B (red), GFP::LGG-1 (green), and LysoTracker Blue (blue) in (A). Scale bars: 10 μm. (C) Time-lapse images of the Rh-Cry5B-treated DA2123 animal. The enlarged images of the yellow squares in (B) indicate 2 autolysosomes. Fluorescence images were taken every 15 min (15′). (See also Fig. S5.).

In order to reconfirm the role of HLH-30 in the Cry5B-activated *atg* gene expression, we performed qRT-PCR of these genes in the Cry5B-treated N2 and *hlh-30(tm1978)* mutant animals (Fig. 6G). Our results showed that the expression of all the Cry5B-activated *atg* genes was significantly abolished in the *hlh-30(tm1978)* animals (all $P < 0.01$). Together, our data indicated that HLH-30 is required for the transcription of these Cry5B-activated *atg* genes.

We next analyzed whether Cry5B can activate HLH-30. By feeding the HLH-30 translational reporter strain OP433 [*wgIs433(hlh-30::TY1::EGFP::3xFLAG)*] on Cry5B plates, we found Cry5B can induce the translocation of HLH-30 from the cytosol to the nucleus (Fig. 6H). Moreover, quantitative analysis results indicated that significantly more animals contain nuclear HLH-30::GFP signals in intestinal cells after 1 ($P < 0.01$) and 3 ($P < 0.01$) h exposure to Cry5B compare with the untreated control groups (Fig. 6I). Notably, the total HLH-30::GFP signal intensity was not upregulated by Cry5B in

OP433 animals (Fig. 6J). Together, our data suggested that Cry5B activates HLH-30 by induction of its nuclear translocation, but not through upregulation of its expression.

To genetically reconfirm that the transcription factor HLHL-30 acts in the same pathway with the Cry5B-acivated *atg* genes, we monitored the survival of N2, *lgg-1* overexpression DA2123 animals (*lgg-1(O/E)*, carrying extra copies of the *lgg-1* transgene driven by its endogenous promoter (Fig. S3B), *hlh-30(tm1978)* mutant, and *lgg-1(O/E);hlh-30(tm1978)* on Cry5B plates (Fig. 6K). Consistent with the previous results (Fig. 2C and Fig. 3C), *lgg-1(O/E)* animals were significantly resistant ($P < 0.01$) and *hlh-30(tm1978)* animals were significantly more hypersensitive ($P < 0.01$) than N2 in response to Cry5B killing; however *lgg-1(O/E);hlh-30(tm1978)* animals were also significantly hypersensitive to Cry5B killing compare with N2 ($P < 0.05$) and were as sensitive as *hlh-30(tm1978)* ($P = 0.63$). These results are consistent with the fact that HLH-
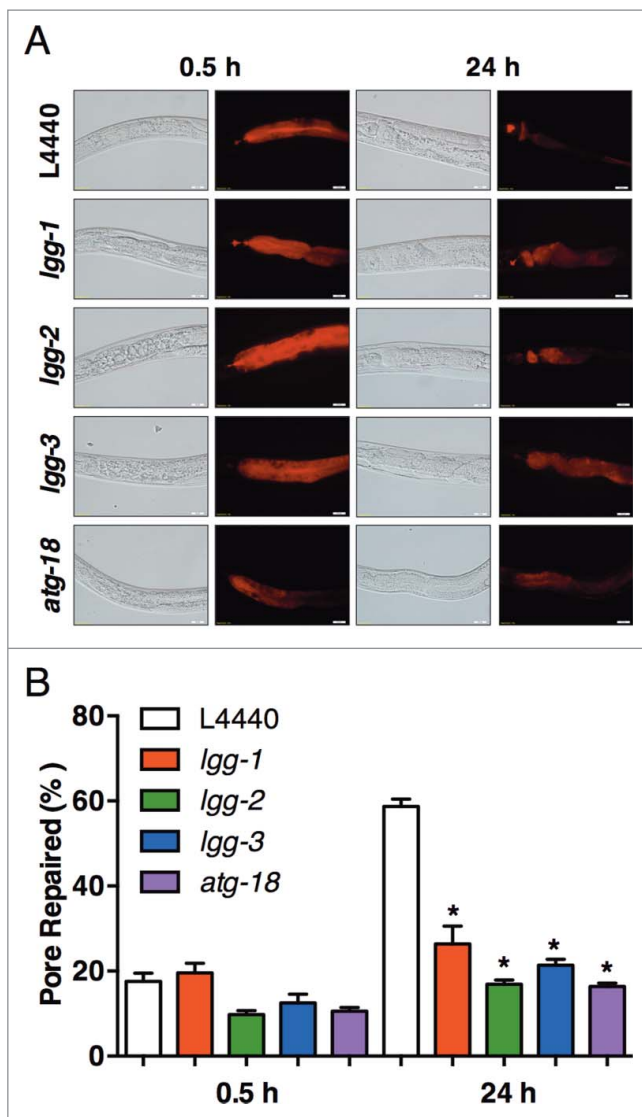
Figure 5. Autophagy is required for intrinsic membrane pore-repair. (A) Representative images of propidium iodide (PI)-treated N2 animals on both Cry5B- and RNAi-expressing *E. coli* plates for 0.5 h, and then transferred to non-Cry5B plates for another 0.5 h or 24 h. L4440 indicates RNAi control. (B) Quantitative analysis of the pore-repaired animals with the PI signals limited in the intestinal lumen. Scale bars: 20 μm. Error bars are SEM.

30 may function as a transcriptional regulator, to mediate Cry5B-activated and *lgg-1*-dependent autophagy.

Finally to test whether *hlh-30* is also required for the intrinsic pore-repair activity, we performed the pore-repair assay by silencing *hlh-30* (Fig. 6L). RNAi of *hlh-30* significantly inhibited the intrinsic pore-repair activity in N2 animals compare with the L4440 control ($P < 0.01$). Taking the above data together, we demonstrated that the transcription factor HLH-30 is activated by Cry5B and is required for the Cry5B-dependent *atg* gene transcription, cellular autophagy activation, and intrinsic membrane pore-repair to defend against Cry5B intoxication in *C. elegans*.

HLH-30-mediated autophagy is generally required for PFT defense in *C. elegans*

To test whether the HLH-30-dependent autophagy is generally required for INCED against bacterial pore-forming toxins, first we fed *C. elegans* with Cry21A-expressing *E. coli*. Cry21A also

perforates the plasma membrane of intestinal cells via a different receptor than Cry5B and intoxicates *C. elegans*.[8] We fed DA2123 animals on Cry21A plates to monitor the upregulation of *lgg-1* expression and the activation of cellular autophagy in *C. elegans* (Fig. S6A). The green fluorescence signal of GFP:: LGG-1 was predominantly and significantly increased in the intestinal cells of animals feeding on Cry21A plates ($P < 0.01$) compare with those on control plates (Fig. S6A and B). Moreover, the Cry21A-treated animals had significant intestinal multiple cytosolic LGG-1 puncta ($P < 0.01$) compare with the control group (Fig. S6A and C). These results demonstrated that Cry21A also activates autophagy in *C. elegans*. Moreover, DA2123 animals were significantly resistant ($P < 0.01$) and *atg-18(gk378)* animals were hypersensitive ($P < 0.01$) to killing by Cry21A compare with N2 animals (Fig. S6D), indicating that autophagy is generally required for Cry PFT defense.

To confirm the role of HLH-30 in PFT-activated autophagy and INCED against Cry21A intoxication, we fed N2 and *hlh-30 (tm1978)* animals on Cry21A plates and monitored their survival ratio (Fig. S6E). Our results showed that the *hlh-30(tm1978)* mutant is significantly hypersensitive to Cry21A compare with N2 ($P < 0.01$). We further tested whether Cry21A also activates HLH-30. By feeding the OP433 animals on Cry21A plates, we found Cry21A also induces the nuclear localization of HLH-30 (Fig. S6F). Moreover, quantitative analysis results indicated that significantly more animals contain intestinal HLH-30::GFP nuclear signals after 1 h exposure to Cry21A compare with the untreated control groups ($P < 0.01$) (Fig. S6G), and the total HLH-30::GFP signal intensity was neither upregulated by Cry21A ($P = 0.65$) (Fig. S6H) as Cry5B (Fig. 6J).

Recombinant streptolysin O (SLO), a cholesterol-dependent PFT with different pore-size (larger) and pore-formation mechanism than Cry toxins, can also intoxicate *C. elegans*.[6] To extend our notion that autophagy is required for bacterial PFT defense; we fed the *C. elegans* with recombinant SLO for 6 d and monitored their survival ratio (Fig. S7). DA2123 animals were significantly resistant ($P < 0.01$) and *atg-18(gk378)* were significantly hypersensitive ($P < 0.01$) to killing by SLO compare with N2 animals, suggesting that autophagy is also required for SLO defense. Overall, our data from Cry5B and Cry21A produced by *Bt* and SLO produced by human-pathogenic *Streptococci* together demonstrated that autophagy is generally required for defense against bacterial PFT in *C. elegans*.

HLH-30 also regulates the transcription of other membrane-repair genes

HLH-30/TFEB has been suggested as an evolutionarily conserved transcription factor in the regulation of various host-defense genes, including autophagy, C-type lectins, lysozymes, and antimicrobial peptides, during bacterial infection.[20] To understand the role of *hlh-30* in Cry5B response, we performed global profiling of whole animal transcriptome by RNA-seq in Cry5B-treated N2 or *hlh-30(tm1978)* animals. We compared the differentially expressed genes (DEGs) between upregulated DEGs in N2-Cry5B/N2-untreated control data set, downregulated DEGs in *hlh-30(tm1978)*-Cry5B/N2-Cry5B data set and downregulated DEGs in *hlh-30(tm1978)*-untreated control/N2-untreated control data set, to search the *hlh-30*-dependent
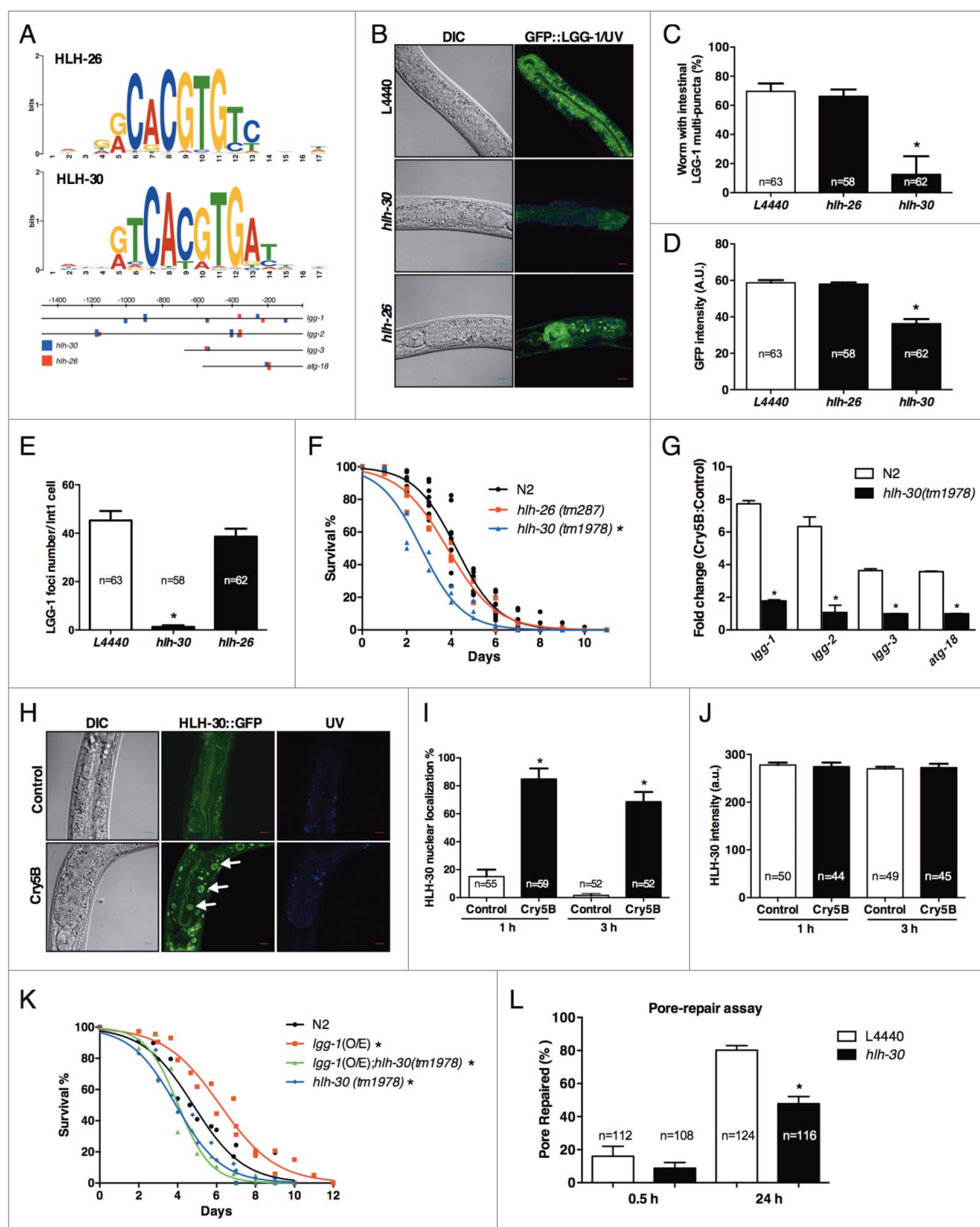
Figure 6. HLH-30 is required for the expression of Cry5B-activated *atg* genes. (A) The consensus motif and the potential binding sites of the HLH-26 and HLH-30 on the Cry5B-activated *atg* genes. (B) Representative confocal images of DA2123 animals on both Cry5B- and RNAi-expressing *E. coli*. L4440 indicates the RNAi control. The confocal images of the GFP::LGG-1 signals (GFP::LGG-1, in green) and the autofluorescence signals (UV, in blue) were overlaid (GFP::LGG-1/UV), and differential interference contrast/Nomarski images (DIC) are also presented. (C) Quantitative analysis of animals with intestinal GFP::LGG-1 cytosolic puncta. (D) Quantitative analysis of the total GFP::LGG-1 signal. (E) Quantitative analysis of the GFP::LGG-1 foci number in the Int1 intestinal cells. (F) Survival analysis of N2, *hlh-26(tm287)*, and *hlh-30(tm1978)* animals feeding on Cry5B plates. (G) qRT-PCR analysis of the Cry5B-activated *atg* genes in N2 and *hlh-30(tm1978)* animals fed with Cry5B for 3 h. (H) Representative DIC and confocal images of OP433 [HLH-30::GFP] transgenic animals on Cry5B plates for 1 h. The confocal images of the HLH-30::GFP signals (HLH-30::GFP, in green) and the autofluorescence signals (UV, in blue), and the DIC images are presented. (I) Quantitative analysis of animals with nuclear HLH-30::GFP in intestinal cells. (J) Quantitative analysis of the total HLH-30::GFP signal. (K) Survival analysis of N2, DA2123 [*lgg-1(O/E)*], *lgg-1(O/E);hlh-30(tm1978)*, and *hlh-30(tm1978)* animals feeding on Cry5B plates. (L) Quantitative analysis of the pore-repaired animals with the PtdIns signals limited in the intestinal lumen. L4440 indicates RNAi control. Scale bars: 10 μm. Error bars are SEM n indicates total animals analyzed. $^{*}P < 0.05$. A.U., arbitrary units. (Also see Fig. S6.).
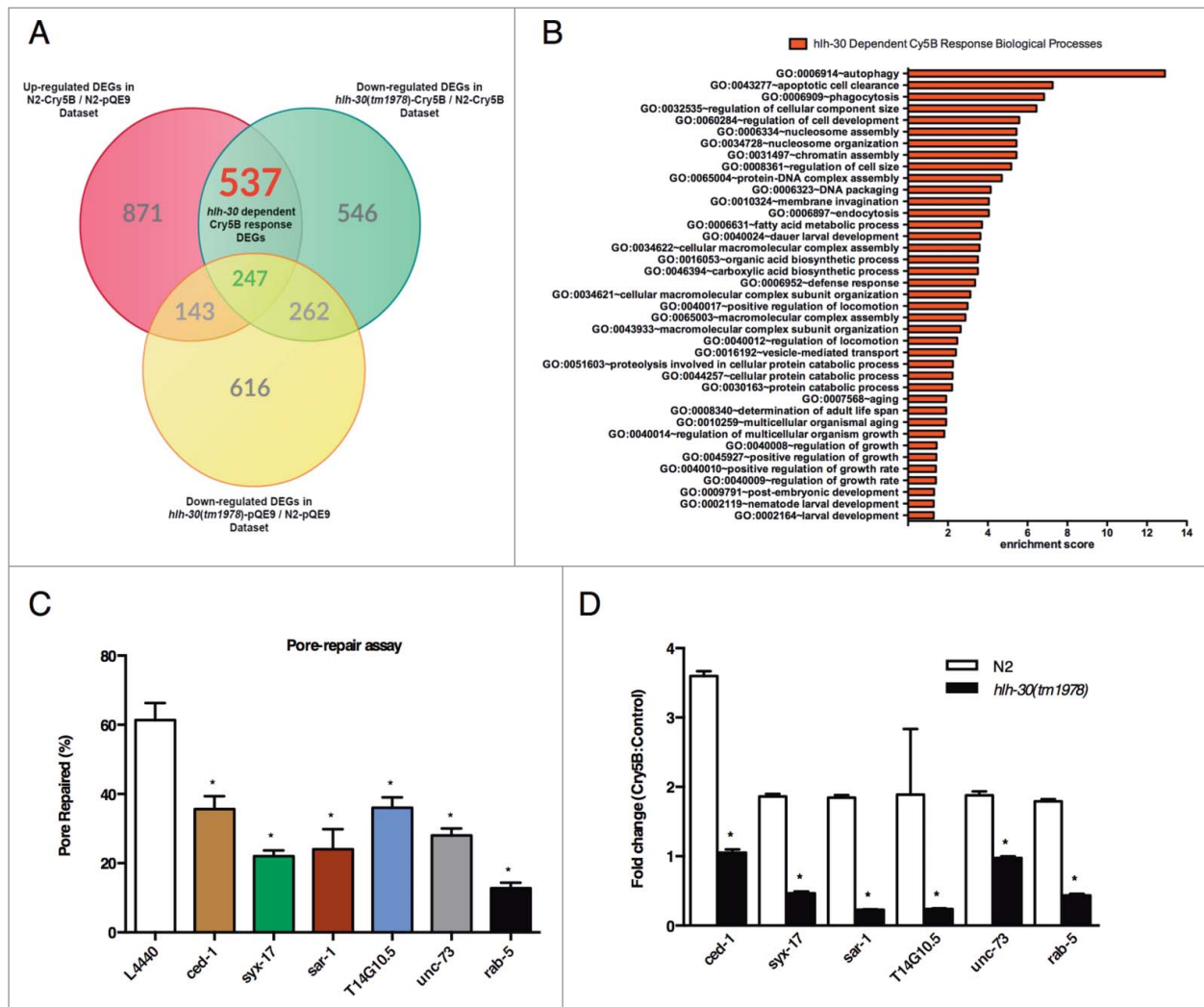
Figure 7. HLH-30 also controls the expression of membrane-repair genes. (A) The Venn diagram of the differentially expressed genes (DEGs) and the *hlh-30*-dependent Cry5B response genes. pQE9 indicates the Cry5B-untreated control. (B) The DAVID GO analysis of the *hlh-30*-dependent Cry5B response genes. (C) Quantitative pore-repair analysis of N2 animals with knockdown of selected *hlh-30*-dependent Cry5B response genes. L4440 indicates RNAi control. (D) qRT-PCR analysis of the *hlh-30*-dependent Cry5B response genes in N2 and *hlh-30(tm1978)* animals fed with Cry5B for 3 h. Error bars are SEM. *$P < 0.05$. (See also Table S1 and S2.).

genes specifically involved in Cry5B response. By this approach, we identified 537 *hlh-30*-dependent Cry5B response genes (Fig. 7A and Table S1). We further applied DAVID GO analysis to this group of genes, and our results indicated that *hlh-30* plays an important role in regulation of autophagy when under Cry5B challenge (Fig. 7B), which is in concordance with our previous conclusions suggested by the results in Figure 6.

It has not escaped our notice that besides autophagy regulation, these genes are also enriched in categories involved in vesicle-mediated transport, endocytosis, and membrane invagination, suggesting possible roles of these genes in Cry5B INCED (Table S2). Among them, the *rab-5* gene has been reported to play an important role in intrinsic membrane-pore repair.[9] Given that *hlh-30* is also required for the intrinsic membrane-pore repair against Cry5B PFT (Fig. 6L), we examined whether the *hlh-30*-dependent Cry5B response genes in these categories are required for intrinsic membrane-pore repair. Among the genes tested, RNAi of the *ced-1/MEGF11, syx-17/SYNTAXIN 17, sar-1/SAR1, T14G10.5/COPG2, unc-73/TRIO,* and *rab-5/RAB5* all conferred significant (all $P < 0.01$) impairment of the intrinsic membrane-repair activity against

Cry5B intoxication (Fig. 7C). In order to reconfirm that these are the *hlh-30*-dependent Cry5B response genes, we performed qRT-PCR analysis (Fig. 7D). Our results demonstrated that the activation of these genes by Cry5B was significantly abolished in the *hlh-30(tm1978)* animals compare with N2 (all $P < 0.01$). Together, our data suggested that HLH-30/TFEB not only regulates cellular autophagy but also controls intrinsic membrane-pore repair systems in response to Cry5B PFT intoxication.

Discussion

Pore-forming toxins (PFTs) comprise a large, structurally heterogeneous group of bacterial protein toxins[2] and PFT targeted cells can mount complex cellular responses to survive from membrane damage.[31] Here, we demonstrated that PFT-elicited autophagy functions cell-autonomously to regulate tolerance to PFT intoxication, via xenophagic degradation of PFT and repair of damaged membrane in *C. elegans*. A model summarizing our findings is shown in the Figure 8. The elevation of autophagic activity by Cry PFTs was, at least in part, reflected at the transcriptional level of the autophagy-related genes, *lgg-1/LC3/ATG8, lgg-2/LC3/ATG8, lgg-3/*
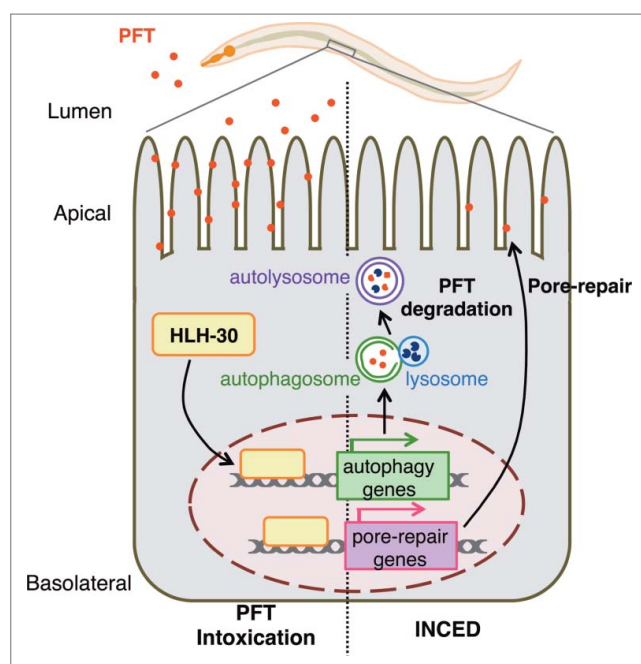
Figure 8. Schematic illustrating relationship between HLH-30-mediated autophagy and epithelium intrinsic cellular defense (INCED) against PFT. Here, we demonstrated that bacterial pore-forming toxin (PFT) triggers autophagy in *C. elegans*. Autophagy is activated by PFT through the transcription factor HLH-30/TFEB. Moreover, autophagy functions cell-autonomously to regulate tolerance to PFT intoxication, via xenophagic degradation of PFT and repair of damaged membrane.

ATG12, and *atg-18/WIPI*, in an *hlh-30/TFEB*-dependent manner. Besides autophagy regulation, HLH-30 can also regulate the expression of other membrane-repair genes in response to PFT attack. Together, our results suggested a role of HLH-30/TFEB-mediated autophagy in epithelium intrinsic cellular defense (INCED) against the most common mode of bacterial virulence factor, bacterial pore-forming toxin, in vivo.

Host cellular autophagy can be either a friend or foe to bacterial pathogens.[13] Autophagy selectively targets some intracellular bacterial pathogens to restrict their growth either in the cytosol or in vacuoles.[32,33] In this scenario, autophagy serves as an innate immune mechanism against bacterial infection. Interestingly, some other intracellular bacterial pathogens have deployed virulence mechanisms, including PFT, to escape this intrinsic cellular defense system or even hijack the autophagy machinery to promote their intracellular growth.[34,35] Our study here demonstrated that recombinant PFTs alone, free from the extracellular bacterial pathogens, can elicit autophagy and the activated autophagy is required for the epithelium INCED and can control host susceptibility through xenophagic degradation of PFT and repair of the perforated membrane. As mentioned previously, autophagy also controls the host susceptibility to various PFTs in cell culture and mouse models.[21,23] Therefore, a logical extension of our and others' findings is that significant therapeutic benefit against a wide range of extracellular bacterial pathogens that utilize PFTs as the major virulence factor could be achieved by upregulation of autophagy. We showed a proof-of-principle that a small molecule autophagy inducer can serve as therapeutics or adjuvant for infections of bacteria expressing PFTs. Besides, since Cry toxins are being tested as novel anthelmintic reagents against animal and human parasitic diseases,[36] a combination treatment of Cry protein and an autophagy inhibitor

may be a suitable regimen for enhancing the therapeutic effects and reducing the possibility of the development of drug resistance from the usage of single Cry PFT.

Pathogenic bacteria produce virulence factors, also known as effectors, which are of importance to the infection process. Host cells possess the evolutionarily conserved effector-triggered immunity (ETI), initially identified in plants, to sense the pathogen through the activity of its effectors and mount a robust immune response. It has been suggested that *C. elegans* also mounts ETI induced by a damage signal, i.e., translational inhibition.[37,38] The ETI is also activated by surveillance pathways overseeing the other core cellular activities of the proteasome, nucleosome, cytoskeleton, and mitochondria, and allows *C. elegans* to detect invading pathogens that deploy effectors to undermine these vital host functions.[39,40] Moreover, HLH-30 mediates early innate immune responses, including antimicrobial and autophagy gene expression, which leads to tolerance to *Staphylococcus aureus* infection.[20] *S. aureus* is also an extracellular pathogen that produces a PFT, α-toxin, however the virulence factor that activates HLH-30 and innate immune responses by *S. aureus* remained unidentified in *C. elegans*. Given that α-toxin also induces autophagy in a cell culture model,[22] testing whether α-toxin is required for *S. aureus* to activate HLH-30-dependent autophagy and ETI is warranted. Moreover, our transcriptomic analysis of the *hlh-30*-dependent Cry5B PFT response genes, also identified genes, including C-type lectins (*clec-62, clec-63, clec-65, clec-186*, and *clec-264*), lysozyme (*lys-8*), *smk-1*, heat shock proteins (*hsp-43, F08H9.3*), M60.2, *prx-11*, and *daf-16* (Table S1 and S2), which are involved in defense response (Fig. 7B). These results are in agreement with the report suggested that HLH-30 regulates cytoprotective and antimicrobial genes.[20] Together with these findings, we may add the disruption of plasma membrane integrity by PFT as a signal cue for ETI and HLH-30 as a surveillance system for this specific effector.

In summary, we have specifically identified the transcription factor HLH-30/TFEB and cellular autophagy as components of epithelium INCED against bacterial PFT in vivo. The divergent pathways and autophagy regulated by HLH-30/TFEB in protective responses reveal how studying pathogenesis can uncover a wonderful complexity and new connections among intracellular pathways. These observations not only advance our knowledge of PFT pathogenesis in *C. elegans*, but also show that the *C. elegans*-PFT model can shed light on the evolutionarily conserved mechanisms of the intrinsic epithelial host defense.

Materials and methods

C. elegans and bacterial strains

C. elegans strains were maintained on NG plates using *E. coli* strain OP50 as the food source under standard conditions.[41] The *C. elegans* strains, including wild-type Bristol strain N2, *glp-4(bn2), bec-1 (ok691), bec-1(ok700), atg-4.1(tm4364), atg-4.2(tm3948), atg-18 (gk378), hlh-26(tm287), hlh-30(tm1978)*, NL2099 *rrf-3(pk1426)*, DA2123 *adIs2122[lgg-1p::lgg-1-GFP + rol-6(su1006)]*,[42] VP303 *rde-1(ne219);kbIs7[nhx-2p::rde-1 + rol-6(su1006)]*,[30] OP433 *unc-119(tm4063);wgIs433[hlh-30::TY1::EGFP::3xFLAG + unc-119 (+)]*,[43] VK1241 *vkEx1241[nhx-2p::mCherry::lgg-1 + myo-2p:: GFP]*,[44] and HZ946 *rpl-43(bp399);bpIs151(SQST-1::GFP)*[27] were ordered from the *Caenorhabditis* Genetics Center (funded by the

National Institutes of Health-Office of Research Infrastructure Programs P40 OD010440, USA) or from the Mitani Lab through the National Bio-Resource Project of the MEXT (Japan). HY0652 *bre-3(ye28)* was created as described.[45] YW364 *lgg-1p::lgg-1::GFP; rol-6 (su1006)* was from Yi-Chun Wu (National Taiwan University, Taiwan). YQ027 *atg-4.1(tm4364);atg-4.2(tm3948)* and YQ280 *adIs2122;hlh-30(tm1978)* were made by the standard genetic method.[41] YQ093 *atg-18(gk378);wfIs118(app-1p::atg-18)* and YQ095 *atg-18(gk378);wfIs120(app-1p::atg-18)* were created by biolistic bombardment[46] of the *app-1p::atg-18::unc-54* transgene into *atg-18(gk378)* background. YQ242 *atg-18(gk378);wfIs231(app-1p:: mCherry::Histone H2B)* and YQ243 *atg-18(gk378);wfIs232(app-1p::mCherry::Histone H2B)* were created by biolistic bombardment of the *app-1p::mCherry-Histone H2B::unc-54* transgene into *atg-18 (gk378)* background. Bacteria expressing dsRNA, including *hlh-26, hlh-30, bre-3, atg* genes (*lgg-1, lgg-2, lgg-3, atg-10,* and *atg-18*), and membrane-repair genes (*ced-1, syx-17, sar-1, T14G10.5, unc-73,* and *rab-5*), were part of the Ahringer RNAi library[47] and the ORFeome-Based RNAi Library[48] in *E. coli* strain HT115 from Geneservice (Cambridge, UK) and Open Biosystems (Huntsville, AL, USA) respectively. All RNAi clones have been confirmed by plasmid DNA sequencing. *E. coli* strain OP50 expressing Cry5B or Cry21A, by transformation of Cry5B and Cry21A expression plasmids (pQE9-Cry5B or Cry21A[3]) respectively, were used in Cry PTFs toxicity experiments. All bacterial strains were cultured under standard conditions.[49]

Media and chemicals

All chemicals used for nematode culture and bacterium culture were from Sigma-Aldrich (NaCl [7647–14–5]; cholesterol [57–88–5]; MgSO$_4$ [10034–99–8]; CaCl$_2$ [10035–04–8]; KH$_2$PO$_4$ [7778–77–0]; K$_2$HPO$_4$ [7758–11–4]) or BD (peptone [211820]; tryptone [211699]; yeast extract [212750]). Spermidine was from Sigma-Aldrich (124–20–9), LysoTracker Blue DND-22 was from Life Technologies (L-7525), and Recombinant SLO protein was from Sigma-Aldrich (401470–29–9).

RNA interference (RNAi)

E. coli strain HT115 transformed with RNAi plasmids were spread on NG-IC plates, which correspond to NG plates (NaCl, peptone, yeast extract, agar, cholesterol, MgSO$_4$ CaCl$_2$ phosphate buffer [KH$_2$PO$_4$, K$_2$HPO$_4$, pH 6] prepared as described previously[41]) with 25 μg/ml carbenicillin (Sigma-Aldrich, 4800–94–6) and 0.1 mM isopropyl-β-D-1-thiogalactopyranoside (MDBio, 101–367–93–1) and incubated at 25°C overnight to induce the dsRNA expression. *E. coli* HT115 with L4440, an empty vector, was used as negative control of RNAi. Synchronized *rrf-3(pk1246)* L1 larvae were obtained using standard protocols,[49] then cultured on L4440 and the autophagy related genes dsRNA expressing RNAi plates at 20°C until L4-young adult stage. These L4-young adult stage worms were transferred to either control plates with *E. coli* that did not express Cry toxins (pQE9 empty vector; Qiagen, 32915) or plates prepared with *E. coli* expressing Cry5B or Cry21A together with *E. coli* either carrying RNAi plasmids or the L4440 plasmid and then incubated at 25°C. The mortality of worms were recorded and analyzed as described previously.[49]

C. elegans autophagy analysis and microscopy

All autophagy analyses were performed according to established guidelines.[26,50] Light microscopic analysis of autophagy: The synchronized L4-young adult stage DA2123 animals carrying the transgene that expresses a GFP::LGG-1 fusion were fed on Cry5B-expressing *E. coli* (pQE9-Cry5B) plates or control (pQE9 vector) plates for 3 h and collected. GFP signals in the animals were acquired by a Nikon Eclipse Ti inverted microscope system (Tokyo, Japan). The GFP intensity, percentage of animals with GFP-positive puncta, and GFP::LGG-1 foci number in the Int1 (the first anterior ring of intestine) cells were determined. For the HLH-30::GFP images, OP433 animals were fed on Cry5B or control plates for 1 and 3 h and collected. For the SQST-1::GFP images, HZ946 animals were fed on Cry5B or control plates for 3 h and collected. Confocal microscopy was performed as described.[24] The L4-young adult stage N2, *bre-3(ye28)* or DA2123 animals were incubated with 50 μg/ml recombinant Cry5B (Rh-Cry5B; generated as described previously[24]), heat-inactivated Cry5B or BSA labeled with rhodamine (Thermo Fisher Scientific, 53031) in a 48-well plate for 3 h. The images were acquired with an Olympus microscope (FV1000MPE, Tokyo, Japan). Time-lapse confocal images of L4-young adult DA2123 animals treated with Rh-Cry5B were acquired with a Zeiss microscope (LSM780, Oberkochen, Germany). LysoTracker Blue was fed during L1 to L4 stage as described.[51] The western blot method for LGG-1 protein was modified by a previously described method.[7] Approximately 750 L4-young adult N2 worms were fed on Cry5B or control plates for 3 h, then worms were removed and washed 3 times in M9 buffer, and sodium dodecyl sulfate (SDS) loading buffer was added. Ten microliters of boiled lysate were used for immunoblotting. Monoclonal antibodies to LC3/LGG-1 (Novus, NB100–2220) and to TUBA/α-tubulin (Sigma- Aldrich, T6199) were used. The relative levels of PE-conjugated LGG-1 and TUBA/α-tubulin were calculated by densitometry using ImageJ (National Institutes of Health). The transmission electron microscopy (TEM) method for autophagy in *C. elegans* was performed using a Hitachi transmission electron microscope (H-7650, Tokyo, Japan) as described previously.[32]

Quantitative Cry PFTs susceptibility

All assays were performed at 25°C and modified by previously described methods,[47] and each assay was performed independently at least 3 times. In brief, the L4-young adult stage worms were fed either on control plates with *E. coli* OP50 that did not express Cry PFT (pQE9 vector control) or on plates prepared with *E. coli* OP50 expressing Cry PFT (pQE9-Cry5B or Cry21A). The mortality of worms on each plate was scored every 24 h. Animals were scored at the indicated times and considered dead upon failure to respond to touch. Animals missing from the agar plate were censored on day of loss. Animal survival was normalized and plotted as a nonlinear regression curve using the GraphPad Prism 6.0 (San Diego) and the time for 50% of the nematodes to die (LT$_{50}$) was calculated by PROBIT analysis as described.[3,47]

Real-time PCR

Real time RT-PCR was performed as described previously.[7] Induction of the mRNA expression of *atg* genes (*unc-51, lgg-1, lgg-2, lgg-3, atg-3,* and *atg-18*), and membrane-repair genes (*ced-1, syx-17, sar-1, T14G10.5, unc-73,* and *rab-5*), by Cry5B was tested in *glp-4(bn2), N2,* and *hlh-30(tm1978)* animals treated for 3 h on *E. coli* expressing Cry5B or not. The experiment was performed using 3 independent sets of cDNA. Real time RT-PCR was performed on an ABI 7000 Instrument (Applied Biosystems, CA, USA) using SYBR Green detection (Applied Biosystems, 4368708). *eft-2* was used as the real time RT-PCR normalization control.[5] Real-time PCR for the *lgg-1* DNA copy number was performed similarly, except the templates were prepared by RNase-treated DNA samples from N2, DA2123, and YW364 animals.

In silico transcription factor prediction

To identify the putative *cis*-regulatory elements and *trans*-acting factor of the Cry5B-induced autophagy genes, *lgg-1, lgg-2, lgg-3,* and *atg-18*, 500~1,500 base pairs upstream of the coding sequences of these genes were retrieved from WormBase[52] and analyzed by the Regulatory Sequence Analysis Tools (RSAT) (www.rsat.eu).[53] The enriched *cis*-regulatory modules of these 4 sequences were predicted by Oligo-analysis[54] in the RSAT. The enriched consensus sequence was inputted into TOMTOM,[55] a motif comparison tool in the Multiple Em for Motif Elicitation Suite (meme-suite.org),[56] to search the transcription factors that recognize similar motifs of *C. elegans* in JASPAR and UniPROBE databases. The putative binding sites of transcription factors were also predicted by Matrix-scan[57] in RSAT.

Transcriptomic analysis of the hlh-30-dependent Cry5B response genes

L4-young adult stage N2 and *hlh-30(tm1978)* worms were fed on Cry5B or control plates for 1 h. Animals were washed twice by M9, then washed twice with DEPC water, and collected and resuspended with 1 ml TRIzol (Invitrogen, 15596026). Total RNA was extracted and cleaned-up with RNeasy Mini Kit (Qiagen, 74104). RNA-seq was performed with illumina MiSeq. To identify the *hlh-30*-dependent Cry5B response genes, the genes with a *P* value of less than 0.05 were selected as differentially expressed genes for further gene ontology and pathway enrichment analyses using DAVID.[58] The accession number of the results uploaded in GEO is GSE78878.

Data analysis

All experiments were performed a minimum of 3 times independently. Statistical analysis between 2 values was compared with a paired *t* test, and among 3 or more values of one independent variable was done with matched one-way ANOVA with the Tukey post-hoc test and more than 2 independent variables by 2-way ANOVA with the Bonferroni post test. All data analysis was performed using SPSS, ver 13.0 (SPSS, Chicago, IL, USA). Statistical significance was set at $P < 0.05$.

Abbreviations

atg/ATG	autophagy-related (yeast Atg homolog)
bec-1	BECN1 (human autophagy) homolog
bre/Bre	Bt toxin-resistant
Bt	*Bacillus thuringiensis*
C. elegans	*Caenorhabditis elegans*
Cry toxins	crystal toxins
ETI	effector triggered immunity
GFP	green fluorescent protein
GO	gene ontology
hlh/HLH	helix loop helix
hpo/Hpo	Hypersensitive to POre-forming toxin
INCED	intrinsic cellular defense
MAP1LC3/LC3	microtubule-associated protein 1 light chain 3
MAPK	mitogen-activated protein kinase
lgg/LGG	LC3 GABARAP and GATE-16 family
PFT	pore-forming toxin
PI	propidium iodide
Rh-Cry5B	rhodamine-labeled Cry5B toxin
RNAi	ribonucleic acid interference
RNA-seq	ribonucleic acid sequencing
SLO	streptolysin O
TEM	transmission electron microscopy
TFEB	transcription factor EB
TUBA	α-tubulin
qRT-PCR	quantitative real-time PCR
SQST-1	sequestosome 1(SQSTM1)/p62 homolog
UPR	unfolded protein response

References

[1] Aroian R, van der Goot FG. Pore-forming toxins and cellular non-immune defenses (CNIDs). Curr Opin Microbiol 2007; 10:57-61; PMID:17234446; http://dx.doi.org/10.1016/j.mib.2006.12.008

[2] Los FC, Randis TM, Aroian RV, Ratner AJ. Role of pore-forming toxins in bacterial infectious diseases. Microbiol Mol Biol Rev 2013; 77:173-207; PMID:23699254; http://dx.doi.org/10.1128/MMBR.00052-12

[3] Chen CS, Bellier A, Kao CY, Yang YL, Chen HD, Los FC, Aroian RV. WWP-1 is a novel modulator of the DAF-2 insulin-like signaling network involved in pore-forming toxin cellular defenses in Caenorhabditis elegans. PloS One 2010; 5:e9494; PMID:20209166; http://dx.doi.org/10.1371/journal.pone.0009494

[4] Wei JZ, Hale K, Carta L, Platzer E, Wong C, Fang SC, Aroian RV. Bacillus thuringiensis crystal proteins that target nematodes. Proc Natl Acad Sci U S A 2003; 100:2760-5; PMID:12598644; http://dx.doi.org/10.1073/pnas.0538072100

[5] Huffman DL, Abrami L, Sasik R, Corbeil J, van der Goot FG, Aroian RV. Mitogen-activated protein kinase pathways defend against bacterial pore-forming toxins. Proc Natl Acad Sci U S A 2004; 101:10995-1000; PMID:15256590; http://dx.doi.org/10.1073/pnas.0404073101

[6] Kao CY, Los FC, Huffman DL, Wachi S, Kloft N, Husmann M, Karabrahimi V, Schwartz JL, Bellier A, Ha C, et al. Global functional analyses of cellular responses to pore-forming toxins. PLoS Pathog 2011; 7:e1001314; PMID:21408619; http://dx.doi.org/10.1371/journal.ppat.1001314

[7] Bischof LJ, Kao CY, Los FC, Gonzalez MR, Shen Z, Briggs SP, van der Goot FG, Aroian RV. Activation of the unfolded protein response is required for defenses against bacterial pore-forming toxin in vivo. PLoS Pathog 2008; 4:e1000176; PMID:18846208; http://dx.doi.org/10.1371/journal.ppat.1000176

[8] Bellier A, Chen CS, Kao CY, Cinar HN, Aroian RV. Hypoxia and the hypoxic response pathway protect against pore-forming toxins in C. elegans. PLoS Pathog 2009; 5:e1000689; http://dx.doi.org/10.1371/journal.ppat.1000689

[9] Los FC, Kao CY, Smitham J, McDonald KL, Ha C, Peixoto CA, Aroian RV. RAB-5- and RAB-11-dependent vesicle-trafficking pathways are required for plasma membrane repair after attack by bacterial pore-forming toxin. Cell Host Microbe 2011; 9:147-57; PMID:21320697; http://dx.doi.org/10.1016/j.chom.2011.01.005

[10] Feng Y, Yao Z, Klionsky DJ. How to control self-digestion: transcriptional, post-transcriptional, and post-translational regulation of autophagy. Trends Cell Biol 2015; 25:354-63; PMID:25759175; http://dx.doi.org/10.1016/j.tcb.2015.02.002

[11] Mizushima N, Levine B. Autophagy in mammalian development and differentiation. Nat Cell Biol 2010; 12:823-30; PMID:20811354; http://dx.doi.org/10.1038/ncb0910-823

[12] Levine B, Mizushima N, Virgin HW. Autophagy in immunity and inflammation. Nature 2011; 469:323-35; PMID:21248839; http://dx.doi.org/10.1038/nature09782

[13] Huang J, Brumell JH. Bacteria-autophagy interplay: a battle for survival. Nat Rev Microbiol 2014; 12:101-14; PMID:24384599; http://dx.doi.org/10.1038/nrmicro3160

[14] Jin M, Klionsky DJ. Regulation of autophagy: modulation of the size and number of autophagosomes. FEBS Lett 2014; 588:2457-63; PMID:24928445; http://dx.doi.org/10.1016/j.febslet.2014.06.015

[15] Melendez A, Levine B. Autophagy in C. elegans. WormBook 2009:1-26; http://dx.doi.org/10.1895/wormbook.1.147.1

[16] Kovacs AL, Zhang H. Role of autophagy in Caenorhabditis elegans. FEBS Lett 2010; 584:1335-41; PMID:20138173; http://dx.doi.org/10.1016/j.febslet.2010.02.002

[17] Settembre C, Di Malta C, Polito VA, Garcia Arencibia M, Vetrini F, Erdin S, Erdin SU, Huynh T, Medina D, Colella P, et al. TFEB links autophagy to lysosomal biogenesis. Science 2011; 332:1429-33; PMID:21617040; http://dx.doi.org/10.1126/science.1204592

[18] O'Rourke EJ, Ruvkun G. MXL-3 and HLH-30 transcriptionally link lipolysis and autophagy to nutrient availability. Nat Cell Biol 2013; 15:668-76; PMID:23604316; http://dx.doi.org/10.1038/ncb2741

[19] Lapierre LR, De Magalhaes Filho CD, McQuary PR, Chu CC, Visvikis O, Chang JT, Gelino S, Ong B, Davis AE, Irazoqui JE, et al. The TFEB orthologue HLH-30 regulates autophagy and modulates longevity in Caenorhabditis elegans. Nature Commun 2013; 4:2267; PMID:23925298

[20] Visvikis O, Ihuegbu N, Labed SA, Luhachack LG, Alves AM, Wollenberg AC, Stuart LM, Stormo GD, Irazoqui JE. Innate host defense requires TFEB-mediated transcription of cytoprotective and antimicrobial genes. Immunity 2014; 40:896-909; PMID:24882217; http://dx.doi.org/10.1016/j.immuni.2014.05.002

[21] Gutierrez MG, Saka HA, Chinen I, Zoppino FC, Yoshimori T, Bocco JL, Colombo MI. Protective role of autophagy against Vibrio cholerae cytolysin, a pore-forming toxin from V. cholerae. Proc Natl Acad Sci U S A 2007; 104:1829-34; http://dx.doi.org/10.1073/pnas.0601437104

[22] Mestre MB, Fader CM, Sola C, Colombo MI. Alpha-hemolysin is required for the activation of the autophagic pathway in Staphylococcus aureus-infected cells. Autophagy 2010; 6:110-25; PMID:20110774; http://dx.doi.org/10.4161/auto.6.1.10698

[23] Maurer K, Reyes-Robles T, Alonzo F, 3rd, Durbin J, Torres VJ, Cadwell K. Autophagy mediates tolerance to Staphylococcus aureus alpha-toxin. Cell Host Microbe 2015; 17:429-40; PMID:25816775; http://dx.doi.org/10.1016/j.chom.2015.03.001

[24] Griffitts JS, Whitacre JL, Stevens DE, Aroian RV. Bt toxin resistance from loss of a putative carbohydrate-modifying enzyme. Science 2001; 293:860-4; PMID:11486087; http://dx.doi.org/10.1126/science.1062441

[25] Marroquin LD, Elyassnia D, Griffitts JS, Feitelson JS, Aroian RV. Bacillus thuringiensis (Bt) toxin susceptibility and isolation of resistance mutants in the nematode Caenorhabditis elegans. Genetics 2000; 155:1693-9; PMID:10924467

[26] Zhang H, Chang JT, Guo B, Hansen M, Jia K, Kovacs AL, Kumsta C, Lapierre LR, Legouis R, Lin L, et al. Guidelines for monitoring autophagy in Caenorhabditis elegans. Autophagy 2015; 11:9-27; PMID:25569839

[27] Guo B, Huang X, Zhang P, Qi L, Liang Q, Zhang X, Huang J, Fang B, Hou W, Han J, et al. Genome-wide screen identifies signaling pathways that regulate autophagy during Caenorhabditis elegans development. Embo Rep 2014; 15:705-12; PMID:24764321

[28] Kang C, Avery L. Death-associated protein kinase (DAPK) and signal transduction: fine-tuning of autophagy in Caenorhabditis elegans homeostasis. FEBS J 2010; 277:66-73; PMID:19878311; http://dx.doi.org/10.1111/j.1742-4658.2009.07413.x

[29] Eisenberg T, Knauer H, Schauer A, Buttner S, Ruckenstuhl C, Carmona-Gutierrez D, Ring J, Schroeder S, Magnes C, Antonacci L, et al. Induction of autophagy by spermidine promotes longevity. Nat Cell Biol 2009; 11:1305-14; PMID:19801973; http://dx.doi.org/10.1038/ncb1975

[30] Espelt MV, Estevez AY, Yin X, Strange K. Oscillatory Ca2+ signaling in the isolated Caenorhabditis elegans intestine: role of the inositol-1,4,5-trisphosphate receptor and phospholipases C beta and gamma. J Gen Physiol 2005; 126:379-92; PMID:16186564; http://dx.doi.org/10.1085/jgp.200509355

[31] Bischofberger M, Iacovache I, van der Goot FG. Pathogenic pore-forming proteins: function and host response. Cell Host Microbe 2012; 12:266-75; PMID:22980324; http://dx.doi.org/10.1016/j.chom.2012.08.005

[32] Jia K, Thomas C, Akbar M, Sun Q, Adams-Huet B, Gilpin C, Levine B. Autophagy genes protect against Salmonella typhimurium infection and mediate insulin signaling-regulated pathogen resistance. Proc Natl Acad Sci U S A 2009; 106:14564-9; PMID:19667176; http://dx.doi.org/10.1073/pnas.0813319106

[33] Wild P, Farhan H, McEwan DG, Wagner S, Rogov VV, Brady NR, Richter B, Korac J, Waidmann O, Choudhary C, et al. Phosphorylation of the autophagy receptor optineurin restricts Salmonella growth. Science 2011; 333:228-33; PMID:21617041; http://dx.doi.org/10.1126/science.1205405

[34] Checroun C, Wehrly TD, Fischer ER, Hayes SF, Celli J. Autophagy-mediated reentry of Francisella tularensis into the endocytic compartment after cytoplasmic replication. Proc Natl Acad Sci U S A 2006; 103:14578-83; PMID:16983090; http://dx.doi.org/10.1073/pnas.0601838103

[35] O'Seaghdha M, Wessels MR. Streptolysin O and its co-toxin NAD-glycohydrolase protect group A Streptococcus from Xenophagic killing. PLoS Pathog 2013; 9:e1003394; PMID:23762025; http://dx.doi.org/10.1371/journal.ppat.1003394

[36] Hu Y, Georghiou SB, Kelleher AJ, Aroian RV. Bacillus thuringiensis Cry5B protein is highly efficacious as a single-dose therapy against an intestinal roundworm infection in mice. PLoS Negl Trop Dis 2010; 4:e614; PMID:20209154; http://dx.doi.org/10.1371/journal.pntd.0000614

[37] McEwan DL, Kirienko NV, Ausubel FM. Host translational inhibition by Pseudomonas aeruginosa Exotoxin A Triggers an immune

response in Caenorhabditis elegans. Cell Host Microbe 2012; 11:364-74; PMID:22520464; http://dx.doi.org/10.1016/j.chom.2012.02.007

[38] Dunbar TL, Yan Z, Balla KM, Smelkinson MG, Troemel ER. C. elegans detects pathogen-induced translational inhibition to activate immune signaling. Cell Host Microbe 2012; 11:375-86; PMID:22520465; http://dx.doi.org/10.1016/j.chom.2012.02.008

[39] Melo JA, Ruvkun G. Inactivation of conserved C. elegans genes engages pathogen- and xenobiotic-associated defenses. Cell 2012; 149:452-66; PMID:22500807; http://dx.doi.org/10.1016/j.cell.2012.02.050

[40] Pellegrino MW, Nargund AM, Kirienko NV, Gillis R, Fiorese CJ, Haynes CM. Mitochondrial UPR-regulated innate immunity provides resistance to pathogen infection. Nature 2014; 516:414-7; PMID:25274306; http://dx.doi.org/10.1038/nature13818

[41] Brenner S. Genetics of Caenorhabditis-Elegans. Genetics 1974; 77:71-94; PMID:4366476

[42] Kang C, You YJ, Avery L. Dual roles of autophagy in the survival of Caenorhabditis elegans during starvation. Genes Dev 2007; 21:2161-71; PMID:17785524; http://dx.doi.org/10.1101/gad.1573107

[43] Sarov M, Schneider S, Pozniakovski A, Roguev A, Ernst S, Zhang Y, Hyman AA, Stewart AF. A recombineering pipeline for functional genomics applied to Caenorhabditis elegans. Nat Methods 2006; 3:839-44; PMID:16990816; http://dx.doi.org/10.1038/nmeth933

[44] Miedel MT, Graf NJ, Stephen KE, Long OS, Pak SC, Perlmutter DH, Silverman GA, Luke CJ. A pro-cathepsin L mutant is a luminal substrate for endoplasmic-reticulum-associated degradation in C. elegans. PloS One 2012; 7:e40145; http://dx.doi.org/10.1371/journal.pone.0040145

[45] Griffitts JS, Huffman DL, Whitacre JL, Barrows BD, Marroquin LD, Muller R, Brown JR, Hennet T, Esko JD, Aroian RV. Resistance to a bacterial toxin is mediated by removal of a conserved glycosylation pathway required for toxin-host interactions. J Biol Chem 2003; 278:45594-602; PMID:12944392; http://dx.doi.org/10.1074/jbc.M308142200

[46] Praitis V. Creation of transgenic lines using microparticle bombardment methods. Methods Mol Biol 2006; 351:93-107; PMID:16988428

[47] Kamath RS, Fraser AG, Dong Y, Poulin G, Durbin R, Gotta M, Kanapin A, Le Bot N, Moreno S, Sohrmann M, et al. Systematic functional analysis of the Caenorhabditis elegans genome using RNAi. Nature 2003; 421:231-7; PMID:12529635; http://dx.doi.org/10.1038/nature01278

[48] Rual JF, Ceron J, Koreth J, Hao T, Nicot AS, Hirozane-Kishikawa T, Vandenhaute J, Orkin SH, Hill DE, van den Heuvel S, et al. Toward improving Caenorhabditis elegans phenome mapping with an ORFeome-based RNAi library. Genome Res 2004; 14:2162-8; PMID:15489339; http://dx.doi.org/10.1101/gr.2505604

[49] Bischof LJ, Huffman DL, Aroian RV. Assays for toxicity studies in C. elegans with Bt crystal proteins. Methods Mol Biol 2006; 351:139-54; PMID:16988432

[50] Klionsky DJ, Abdelmohsen K, Abe A, Abedin MJ, Abeliovich H, Acevedo Arozena A, Adachi H, Adams CM, Adams PD, Adeli K, et al. Guidelines for the use and interpretation of assays for monitoring autophagy (3rd edition). Autophagy 2016; 12:1-222; PMID:26799652; http://dx.doi.org/10.1080/15548627.2015.1100356

[51] O'Rourke EJ, Soukas AA, Carr CE, Ruvkun G. C. elegans major fats are stored in vesicles distinct from lysosome-related organelles. Cell Metab 2009; 10:430-5; PMID:19883620; http://dx.doi.org/10.1016/j.cmet.2009.10.002

[52] Howe KL, Bolt BJ, Cain S, Chan J, Chen WJ, Davis P, Done J, Down T, Gao S, Grove C, et al. WormBase 2016: expanding to enable helminth genomic research. Nucleic Acids Res 2016; 44:D774-80; http://dx.doi.org/10.1093/nar/gkv1217

[53] Medina-Rivera A, Defrance M, Sand O, Herrmann C, Castro-Mondragon JA, Delerce J, Jaeger S, Blanchet C, Vincens P, Caron C, et al. RSAT 2015: Regulatory Sequence Analysis Tools. Nucleic Acids Res 2015; 43:W50-6; http://dx.doi.org/10.1093/nar/gkv362

[54] van Helden J, Andre B, Collado-Vides J. Extracting regulatory sites from the upstream region of yeast genes by computational analysis of oligonucleotide frequencies. J Mol Biol 1998; 281:827-42; PMID:9719638; http://dx.doi.org/10.1006/jmbi.1998.1947

[55] Gupta S, Stamatoyannopoulos JA, Bailey TL, Noble WS. Quantifying similarity between motifs. Genome Biol 2007; 8:R24; PMID:17324271; http://dx.doi.org/10.1186/gb-2007-8-2-r24

[56] Bailey TL, Boden M, Buske FA, Frith M, Grant CE, Clementi L, Ren J, Li WW, Noble WS. MEME SUITE: tools for motif discovery and searching. Nucleic Acids Res 2009; 37:W202-8; PMID:19458158; http://dx.doi.org/10.1093/nar/gkp335

[57] Turatsinze JV, Thomas-Chollier M, Defrance M, van Helden J. Using RSAT to scan genome sequences for transcription factor binding sites and cis-regulatory modules. Nat Protoc 2008; 3:1578-88; PMID:18802439; http://dx.doi.org/10.1038/nprot.2008.97

[58] Huang da W, Sherman BT, Lempicki RA. Systematic and integrative analysis of large gene lists using DAVID bioinformatics resources. Nat Protoc 2009; 4:44-57; PMID:19131956; http://dx.doi.org/10.1038/nprot.2008.211